Constraint Effects on Thin Film Channel Cracking Behavior

Ting Y. Tsui and Andrew J. McKerrow

*Silicon Technology Development, Texas Instruments Inc, 13560 North Central Express Way, Dallas, TX 75246, U.S.*A.

Joost J. Vlassak

Division of Engineering and Applied Sciences, Harvard University, 311 Pierce Hall, 29 Oxford Street, Cambridge MA 02138

Corresponding Author – Ting Y. Tsui

Email : ttsui@ti.com

Published in J. Mater. Res., Vol. 20, No. 9, Sep 2005

Abstract – One of the most common forms of cohesive failure observed in brittle thin film subjected to a tensile residual stress is channel cracking, a fracture mode in which through-film cracks propagate in the film. The crack growth rate depends on intrinsic film properties, residual stress, the presence of reactive species in the environments, and the precise film stack. In this paper, we investigate the effect of various buffer layers sandwiched between a brittle carbon-doped-silicate (CDS) film and a silicon substrate on channel cracking of the CDS film. The results show that channel cracking is enhanced if the buffer layer is more compliant than the silicon substrate. Crack velocity increases with increasing buffer layer thickness and decreasing buffer layer stiffness. This is caused by a reduction of the constraint imposed by the substrate on the film and a commensurate increase in energy release rate. The degree of constraint is characterized experimentally as a function of buffer layer thickness and stiffness, and compared to the results of a simple shear lag model that was proposed previously. The results show that the shear lag model does not accurately predict the effect of the buffer layer.

I. Introduction

To reduce device size and power consumption, advanced optical and electronic devices are often made of thin-film composite structures. They can be deposited using a range of techniques, such as plasma enhanced chemical vapor deposition (PECVD), high-density plasma deposition (HDP), spin-on coating, and a variety of sputtering methods. Most films are subject to residual stresses. Often films are deposited at temperatures greater than the ambient environment and have thermal expansion coefficients that are different from the substrate material. This mismatch in thermal expansion creates a compressive or tensile residual film stress that sometimes leads to delamination or cohesive fracture [1-6]. In addition to thermal mismatch, residual stresses may also arise from the actual deposition process or as a result of lattice mismatch for epitaxial films.

One common cohesive failure mode for thin films under tension is channel cracking, where through-film cracks propagate in the film [6]. The energy release rate, G, for a channel crack can be calculated using the following equation:

$$G = Z\frac{\pi}{2}\frac{\sigma^2 h}{\bar{E}}, \qquad (1)$$

where h, σ, and $\bar{E} = E/\left(1-\nu^2\right)$ represent the film thickness, residual stress, and plane-strain elastic modulus, respectively. Z is a constant that depends on the elastic mismatch between film and substrate and on the precise geometry. The effect of elastic mismatch on the energy release rate has been calculated by Beuth [7] for channel cracking in a film on a half space and by Vlassak [5] for a film on a substrate of finite thickness. The factor Z can be expressed as a function of the plane-strain Dundurs parameters [5, 7-8]

$$\alpha = \frac{\bar{E}_f - \bar{E}_s}{\bar{E}_f + \bar{E}_s}, \qquad \beta = \frac{\mu_f(1-2\nu_s) - \mu_s(1-2\nu_f)}{2\mu_f(1-\nu_s) + 2\mu_s(1-\nu_f)}, \tag{2}$$

where μ represents the shear modulus and ν Poisson's ratio. The subscripts correspond to film (f) or substrate (s) properties. Figure 1 shows a graph of Z calculated by Beuth [7] as a function of α with $\beta = \alpha/4$ for a film on a half space. The figure shows that Z does not vary significantly when α is negative, i.e., for a compliant film on a stiff substrate. If α is greater than zero, however, the film is stiffer than the substrate and Z increases rapidly. This suggests that the driving force for channel cracking is relatively insensitive to the substrate properties when a compliant film is deposited on a stiff substrate. In contrast, the energy release rate changes quickly if the same film is bonded to a substrate that is more compliant than the film. This strong dependence on α is important for the following reason. When a film of a given thickness is deposited on a stiff substrate, the residual stress in the film may be insufficient to drive a channel crack. If the same film is deposited on a more compliant substrate, however, the energy release rate may well exceed the fracture toughness of the film making it vulnerable to channel cracking and failure. This observation applies to a monolithic substrate, but one can expect qualitatively similar behavior if a thin film of a compliant material is deposited prior to deposition of the film of interest. The compliant film acts as a buffer between film and substrate, and has the effect of reducing the constraint by the substrate, in effect increasing the apparent value of α.

Even when the driving force for channel cracking is less than the fracture toughness of the film, channel cracking may occur if there is a chemical species in the environment that reacts with the strained bonds at a crack tip. This phenomenon is known as subcritical or environmentally aided fracture. If crack growth is controlled by the reaction at the crack tip, the crack growth velocity, V, depends sensitively on the strain energy release rate in the film. Both

experiments and physical models suggest an exponential relationship between crack velocity and energy release rate [6-9]:

$$V = V_o e^{\left(\frac{G}{2NkT}\right)}, \tag{3}$$

where k is the Boltzmann constant, T the absolute temperature, N the bond density, and V_o a reference velocity. Combining equations (1) and (3) results in the following expression for the crack velocity

$$V = V_o\, e^{\left(\frac{Z\pi\,\sigma^2 h}{4\bar{E}NkT}\right)}. \tag{4}$$

Equation (4) shows that, for a constant film stress, the crack velocity increases exponentially with film thickness, *h,* and constraint factor *Z*. Crack velocity is thus a sensitive measure of the effect of the substrate constraint on the energy release rate.

In this article, the constraint effect of buffer layers on channel crack propagation is investigated for tensile carbon-doped silicate (CDS) coatings. This is achieved by measuring crack velocity for subcritical crack growth in a constant-humidity environment. Samples with underlying films that are either stiffer or more compliant than CDS are investigated. It is demonstrated that the energy release rate and hence channel crack growth depend strongly on the elastic properties and thickness of the under-lying layer.

II. Experimental Procedure

II.a. Thin Film Deposition

Tensile carbon-doped silicate (CDS) films were deposited using plasma-enhanced chemical vapor deposition (PECVD) near 400°C. Tetra-methylcyclo-tetrasiloxane (TMCTS) was used as the silicon and carbon source for the film. The precursor was mixed with oxygen gas in the

deposition chamber to form a carbon-doped silicate. Films of CDS deposited on 200 mm diameter (100) silicon substrates have a residual tensile stress of approximately 60 MPa, independent of film thickness, as measured using the substrate curvature technique. The CDS films contain Si, O, H, and C, with a composition of 22, 36, 28, and 14 at %, respectively. FTIR spectrum analysis reveals that the carbon atoms are predominantly incorporated as methyl groups bonded to Si atoms, disrupting the Si-O network structure. The film density as measured by the Rutherford Backscattering Spectrometry (RBS) technique is 1.20 g/cm^3, which is approximately half the density of fused silica. The elastic modulus and hardness of the CDS were measured using nanoindentation and were found to be 8 GPa and 1.5 GPa, respectively.

Channel cracks were viewed in cross-section using scanning electron microscopy (SEM). Samples were prepared by cleaving the substrate perpendicular to the channel crack with a maximum rotational error of approximately 15 degrees. The estimated linear error because of rotational misalignment of the cracks is less than 4 %; the error in magnification is less than $\pm$5 % of the true value.

To study the substrate constraint effect on channel cracking, thin films with different elastic modulus values were deposited on bare (100) silicon substrates prior to deposition of the CDS films. The under-layers include silicon nitride (SiN_x), tetra-ethoxysilane (TEOS) silicon dioxide (SiO_2), octa-methylcyclo-tetrasiloxane (OMCTS) low-density carbon-doped silicon oxide (LD-CDO), and a poly-aromatic polymer. A summary of the mechanical properties of the under-layers is given in Table 1. The elastic moduli were measured with nanoindentation, the residual stress with the substrate curvature technique. The elastic moduli of these materials vary over a wide range from approximately 3 to 160 GPa. Thus, the under-layer materials used in this study include both materials that are stiffer and more compliant than the CDS. All films except the

organic polymer were deposited in the temperature range from 350°C to 400°C using PECVD. The polymer films were spin-coated under ambient conditions with a final anneal in forming gas at 400°C for 30 minutes.

II.b. Channel Crack Velocity Measurements

Channel crack growth in CDS films was studied in a controlled air environment at a temperature of 21±2°C. Cracks were induced by scratching samples with a sharp diamond scribe. Scratch depths were greater than the film thickness and the length of the scratches was approximately 10 mm. Samples were then stored in a controlled environment with a relative humidity in the range of $40 \pm 5\%$ allowing the cracks to propagate. After specific periods of time, crack lengths were measured using an optical microscope. The time delay between crack initiation and length measurements depended on the propagation speed of the crack and could be as much as several months for very slow cracks. Only cracks with lengths exceeding 30 times the film thickness were considered to minimize any effects of the residual stress fields around the scratches used to nucleate the cracks. Each crack velocity was calculated as the average velocity of at least ten channel cracks measured on a given sample. Unless otherwise stated, all crack velocity data in this work were obtained using this method.

III. Results and Discussions

III.a. Channel Crack Geometry

Figure 2 shows a typical cross-section scanning electron micrograph of a channel crack in a 3.42 μm CDS coating deposited on a bare silicon substrate. Figure 2 reveals no delamination between CDS film and substrate. The crack is approximately 0.13 μm wide at the film surface and has a depth of 3.27 μm. A high-magnification image of the crack tip near the interface is

shown in Fig. 3. Interestingly, it shows that the crack does not terminate at the interface. Instead, the crack tip is located approximately 0.16 μm from the interface. This behavior was predicted by Beuth [7] in his analysis of channel cracking. Based on his calculations, he proposed that when a compliant material such as CDS is deposited on a stiff substrate such as Si, channel cracks would terminate within the film rather than at the interface. Beuth showed that for Dundurs parameters $\alpha = -0.80$ and $\beta = \alpha/4$, the energy release rate is greatest for a crack depth to film thickness ratio (*a/h*) of ~0.96. The sample under consideration has an α value of -0.91. Thus, the maximum of the energy release rate should occur at a slightly smaller value of *a/h*. This implies that channeling cracks in this sample should have a depth of *at least* that value. The micrograph in Fig. 3 reveals an a/h ratio of 0.97, which is indeed within the expected range.

In order to confirm that termination of the CDS channel cracks within the film is due to the elastic constraint imposed by the substrate, a 0.42 μm polymer film was spin-coated on a bare silicon substrate prior to the CDS deposition. The polymer film was used because with an elastic modulus of 3.5 GPa it is more compliant than both the silicon and the CDS. It acts as a buffer layer that reduces the effective elastic constraint experienced by the CDS film. According to Beuth, this allows the crack to propagate further toward or even through the interface. Figures 4 and 5 show an SEM cross-section of a channel crack in the CDS/polymer/silicon substrate sample. The micrographs reveal that the crack has propagated past the CDS/polymer interface and into the polymer film. This confirms that the crack arrest observed in Figs. 2 and 3 can be attributed to the presence of the stiff silicon substrate.

The crack tip opening provides information on the driving force for channel cracking. The crack opening displacement is plotted in Fig. 6 as a function of distance to the crack tip for the

CDS film on bare silicon. Beuth [7] has shown that the constraint parameter, Z, can be calculated from the crack opening geometry using the following equation

$$Z = \frac{\int_0^a \delta(y)\, dy}{\pi \frac{\sigma}{\bar{E}_{film}} a\, h}. \qquad (5)$$

By integrating the crack opening displacement in Fig. 6 and using the material properties listed in Table 1, the constraint factor for CDS deposited on silicon is determined to be 0.73. This value is within 1% of the value predicted by Beuth for a material system with α=-0.91 and $\beta = \alpha/4$.

It is important to note that the channel crack penetration depth and the crack opening area reported in this section may be slightly altered by the sample cross-sectioning process. Given the very good agreement between experimental data and theory, however, the effect is likely to be small.

III.b. Channel crack velocity for CDS films on monolithic silicon substrates

Figure 7 shows the crack growth velocity for CDS films deposited on bare silicon substrates as a function of film strain energy release rate. Crack growth rate data were collected over a wide range of velocities from 10^{-4} to 10^{3} μm/sec. The figure shows two distinct regimes in the fracture behavior. At low velocities, the crack growth rate increases exponentially with film thickness. This is an indication that fracture of the CDS films in this velocity range is reaction-rate limited [9-10]. At velocities exceeding 100 μm/s, however, transport of the active species to the crack tip becomes important and the slope of the velocity curve is reduced [9-10]. In the following sections, the data in Fig. 7 will be used as a “master curve” to illustrate the effect of underlying layers on the energy release rate and the corresponding channel crack velocity in CDS films.

III.c. The effect of underlying layers on the energy release rate

In order to quantify the effect of underlying layers on channel crack propagation in CDS, thin films with elastic moduli greater than and smaller than the CDS were used as buffer layers between the silicon substrate and the CDS films. First, the effect of SiN_x and SiO_2 buffer layers will be discussed. Both materials have modulus values greater than CDS, but smaller than silicon. This is followed by two materials – a spin-on organic polymer and low-density carbon-doped-oxide – that have elastic moduli that are approximately two times lower than the CDS modulus.

Crack velocity data for a 3.25 μm CDS film are plotted as a function of SiN_x and SiO_2 layer thickness in Fig. 8. The channel crack velocity for a CDS film of the same thickness deposited on bare silicon is labeled in the figure as a reference. The figure shows that channel cracks grow faster when CDS is deposited on SiN_x or SiO_2 buffer layers, than when deposited directly on Si. The composition and bond structure of the CDS film does not depend on the buffer layer on which it is deposited. Moreover, the residual stress, elastic modulus, and film thickness are the same for all samples. Consequently, the increased crack growth velocity can be attributed to the greater energy release rate applied to the CDS film as a result of the SiN_x and SiO_2 buffer layers. According to Eq. (1), the energy release rate for channel cracking in a film on a monolithic substrate is proportional to the elastic constraint factor, Z, which in turn is determined by the elastic modulus mismatch between film and substrate. If there is a buffer layer that is more compliant than the substrate, such as the SiN_x and SiO_2 layers in the current experiments, the constraint on the cracked film is reduced and the value of Z increases. The result is a larger energy release rate and crack propagation velocity as shown in Fig. 8. CDS films with a SiO_2 buffer layer have greater crack velocities than those with a SiN_x layer, because SiO_2 is more

compliant than SiN_x (e.g., See Table 1). In fact, there is only a minimal increase in crack propagation rate for samples with a SiN_x buffer layer, since the elastic modulus mismatch between SiN_x and silicon is only 4%. As the buffer layer thickness increases, the channel crack velocity approaches a limiting value that corresponds to the velocity of a channel crack in a CDS film deposited on a monolithic substrate made of buffer layer material. The limiting values for SiN_x and SiO_2 were calculated from the master curve in Fig. 7 and the data in Table 1. They are marked by the arrows in Fig. 8 and are in good agreement with the experimental measurements.

The reason why the energy release rate increases with increasing buffer layer thickness is best explained by the schematic illustration shown in Fig. 9. If the buffer layer is more compliant than the substrate, a channel crack will result in relaxation of the film stress over a greater distance than for a crack in a film deposited directly on the substrate. Since it is the change in strain energy associated with the relaxation of the film stress that drives crack growth, samples with a thicker buffer layer also experience a greater energy release rate for channel cracking. As the thickness of the buffer layer increases further, the elastic field associated with the channel crack is fully contained within the buffer layer and the energy release rate approaches that for a film on a substrate with the same elastic properties as the buffer layer.

A rigorous mechanics analysis of channel cracking in systems with a buffer layer would show that the constraint factor depends on the Dundurs parameters for both interfaces as well as on the buffer layer thickness. Such an analysis is beyond the scope of this paper. Rather, insight in the effect of the buffer layer can be gained through use of an "effective substrate modulus", which is calculated from experimental crack velocities. The effective substrate modulus is defined as the plane-strain modulus of a monolithic substrate that results in the same constraint factor as the system with the buffer layer. This effective stiffness depends on the buffer layer

thickness and the elastic constants of the materials involved. It should be noted that this definition is not unique, because the constraint factor depends on both Dundurs parameters. However, for most practical systems, β takes on values between zero and $\alpha/4$, and the constraint factor is only a weak function of β in this range [5, 7]. In order to obtain a unique definition, the second Dundurs parameter β was taken equal to $\alpha/4$, which is close to the value expected based on the mechanical properties listed in Table 1. Since the film stress and thickness are the same for all samples, the crack growth velocities in Fig. 8 can be converted to energy release rates using the data in Fig. 7. Using Equations (1) and (2) combined with the results in Fig. 1, these energy release rates are in turn converted to effective substrate moduli. Figures 10 (a) and (b) show the effective moduli for samples with SiO_2 and SiN_x buffer layers as a function of buffer layer thickness. For the SiO_2 buffer layer, the effective modulus approaches the plane-strain modulus value for Si of 172 GPa, when the buffer layer is very thin, and the value for SiO_2 (75 GPa), when the buffer layer is thick. The trend for the SiN_x buffer layer is the same, but quantitative agreement is not quite as good. This is so because the value of the effective modulus for a compliant film on a stiff substrate depends sensitively on the precise value of α.

Because the CDS film is more compliant than both SiO_2 and SiN_x, these buffer layers have only a relatively small effect on the energy release rate, as one would expect based on Fig. 1. The effect is much more dramatic when the CDS film is deposited on a more compliant buffer layer such as the low-density carbon doped oxide (LD-CDO) or the organic polymer. Both of these materials have elastic modulus values of 3.5 GPa, which is smaller than the CDS modulus of 8 GPa, with a corresponding α value of 0.4. The graph in Fig. 1 suggests that now the constraint factor and the energy release rate should increase significantly with buffer layer thickness. Figure 11 shows the channel crack velocity in a 3.0 μm CDS film as a function of the LD-CDO and

polymer buffer layer thickness. Crack velocity indeed increases rapidly with thickness and the rate of increase is significantly faster than for the samples with SiO_2 and SiN_x buffer layers shown in Fig. 8. With a 0.5 μm LD-CDO under-layer, the crack velocity is approximately four orders of magnitude larger than for CDS deposited on a bare silicon substrate with a value of approximately 100 μm/s. The effective substrate modulus for the LD-CDO buffer is plotted as a function of layer thickness in Fig. 12. The figure clearly shows that the effective modulus decreases very rapidly with buffer layer thickness and that it approaches the LD-CDO plane-strain modulus for buffer layer thicknesses as small as 16% of the CDS thickness.

Rather than using the qualitative effective modulus concept, it is possible and maybe more useful to define a correction factor, *M*, to describe the effect of the buffer layer:

$$M = \frac{Z_{BL}\left(\alpha,\alpha_1,\beta_1,\beta_2,h_{BL}/h_f\right)}{Z_{Mono}(\alpha,\beta)} \approx \frac{Z_{BL}\left(\alpha,\alpha_1,h_{BL}/h_f\right)}{Z_{Mono}(\alpha)}, \qquad (6)$$

where the subscripts BL and Mono refer to systems with a buffer layer and a monolithic substrate respectively. Subscript 1 refers to the CDS/buffer layer interface, and 2 to the buffer layer/substrate interface. Dundurs parameters without subscript refer to the CDS/substrate material couple. For simplicity, the functional dependence on β_1 and β_2 was neglected in Eq. (6). It should be noted that ignoring the effect of the β parameter generally results in an error of less than 10% for a compliant films on stiff monolithic substrate, and a much smaller error for a stiff film on a compliant substrate. Figure 13 shows a compilation of the correction factors as a function of film thickness for all material systems considered in this study. For very small values of h_{BL}/h_f, the correction factor approaches unity, while for large values it approaches $Z_{Mono}(\alpha_1)/Z_{Mono}(\alpha)$.

Suo [12-13] has proposed a simple shear lag model to calculate the driving force for channel cracking as a function of buffer layer thickness. According to this model, the energy release rate and the corresponding correction factor are given by

$$G = \sqrt{\frac{h_{BL}\bar{E}_f}{h_f \mu_{BL}}} \frac{\sigma^2 h_f}{\bar{E}_f} \quad \text{and} \quad M = \frac{1}{Z_{Mono}(\alpha)} \sqrt{\frac{h_{BL}\bar{E}_f}{h_f \mu_{BL}}}, \tag{7}$$

where μ_{BL} is the shear modulus of the buffer layer. The dashed lines in Fig. 14 represent the correction factors for the various buffer layers according to Eq. (7). Agreement with experimental results is fairly poor even for the most compliant buffer layer. This is so because Eq. (7) only considers the effect of the buffer layer, and neglects the contribution of the substrate or non-uniform deformation of the film. As a result, the formula predicts a vanishing energy release rate in the limit of zero buffer layer thickness. In the limit when the buffer layer thickness approaches infinity, the energy release rate grows without bound, which is also unrealistic. It is not surprising that this model does not predict the correct limits since it is based on a shear lag model that highly simplifies the deformation field; it is not based on a rigorous mechanics analysis of the fracture problem. A better fit can be obtained by adding a term equal to $Z_{Mono}^2(\alpha)$ below the square root. This term corrects the problem with the lower limit, but the expression is still not accurate enough to represent the experimental data over a wide range of buffer layer thicknesses. Clearly, a more detailed analysis is needed to describe the channel crack behavior observed in these systems.

IV. Conclusions

It has been demonstrated that the subcritical channel crack growth rate in carbon-doped silicate (CDS) coatings depends sensitively on the elastic properties and thickness of underlying

layers. An underlying layer that is more compliant than the substrate results in an increase of the energy release rate and a corresponding increase in crack velocity. If the underlying layer is stiffer, the energy release rate is reduced and so is the crack velocity. The effect of the underlying layer on the channel cracking energy release rate increases with the thickness of that layer and can be described by means of a correction factor. This correction factor depends on the Dundurs parameters of the interfaces involved and on the thickness of the underlying layer. For very thin layers, the correction factor approaches unity; if the thickness of the underlying layer exceeds the thickness of the coating, the energy release rate for channel cracking approaches the value for the corresponding monolithic substrate. These observations have important implications for the reliability of brittle coatings: In addition to the residual stress, thickness, and fracture toughness of a coating, one also needs to consider the precise film stack to determine whether the coating is prone to channel cracking.

V. Acknowledgments

The authors would like to express their gratitude to Rhida Dalmacio and Darrell Ingram for assisting with the sample preparation. Additional thanks go to the SiTD management for their support of the mechanical reliability program.

References

1. Q. Ma, "A Four-Point Bending Technique for Studying Subcritical Crack Growth in Thin Films and at Interfaces," Journal of Materials Research, **12**, 840-845 (1997)

2. M. Lane, N. Krishna, I. Hashim, and R. H. Dauskardt, "Adhesion and Reliability of Copper Interconnects with Ta and TaN Barrier Layers," Journal of Materials Research, **15** [1] 203-211, (2000)

3. Ting Y. Tsui, A. J. Griffin, Jr., Jeannette Jacques, Russell Fields, Andrew J. McKerrow, and Robert Kraft, "Effects of Elastic Modulus on the Fracture Behavior of Low-Dielectric Constant Films," Proceedings of the 2005 IEEE International Interconnect Technology Conference, Institute of Electrical and Electronics Engineers (IEEE) Electronic Devices Society, Burlingame, California, June 2005.

4. A.A. Volinsky, P. Waters, J.D. Kiely, E. Johns, "Sub-Critical Telephone Cord Delamination Propagation," Mat. Res. Soc. Symp. Proc. Vol. 854E, U9.5 (2004)

5. J.J. Vlassak, "Channel cracking in thin films on substrates of finite thickness," International Journal of Fracture **119** (4), 299-312 (2003)

6. R.F. Cook and E.G. Liniger, "Stress-corrosion cracking of low-dielectric-constant spin-on-glass thin films," Journal of the Electrochemical Society, **146**, 4439-48 (1999)

7. J.L. Beuth Jr., “Cracking of thin bonded films in residual tension,” International Journal of Solids and Structures, **29**, 1657-75 (1992)

8. Dundurs J. “Edge-bonded dissimilar orthogonal elastic wedges,” J. Appl. Mech., **36**, 650-652 (1969)

9. B.R. Lawn, Fracture of Brittle Solids, 2nd ed. (Cambridge Press, Cambridge, 1993).

10. S. M. Wiederhorn and H. Johnson, “Effect of Electrolyte pH on Crack Propagation in Glass,” Journal of The American Ceramic Society, **56** (4), 192 (1973).

11. T. H. Courtney, Mechanical Behavior of Materials, (McGraw-Hill Publishing Company, 1990).

12. Z. Suo, “Reliability of interconnect structures”, in Comprehensive Structural Integrity, Volume 8, Interfacial and Nanoscale Fracture, p 265-324, edited by I. Milne, R.O. Ritchie, and B. Karihaloo (Elsevier, 2003)

13. Jun He, Guanghai Xu, and Z. Suo, “Experimental Determination of Crack Driving Forces in Integrated Structures,” Proceedings of the 7th International Workshop on Stress-Induced Phenomena in Metallization, Austin, Texas, edited by P.SW. Ho, S.P. Baker, T. Nakamura, C.A. Volkert, American Institute of Physics, New York, pp 3-14, June 2004.

Table 1. Material properties of coatings used in this work.

	Elastic modulus (GPa)	Plane-strain modulus (GPa)	Residual stress (MPa)
Si*	163	172	n/a
SiN_x	155	165	-125 +/- 5
SiO_2	70	75	-135 +/- 5
CDS	8.0	8.5	60 +/- 2
Organic polymer	3.5	3.7	60 +/- 2
Low density CDO	3.5	3.7	60 +/- 3

* Polycrystalline values calculated from single-crystal elastic constants [11]

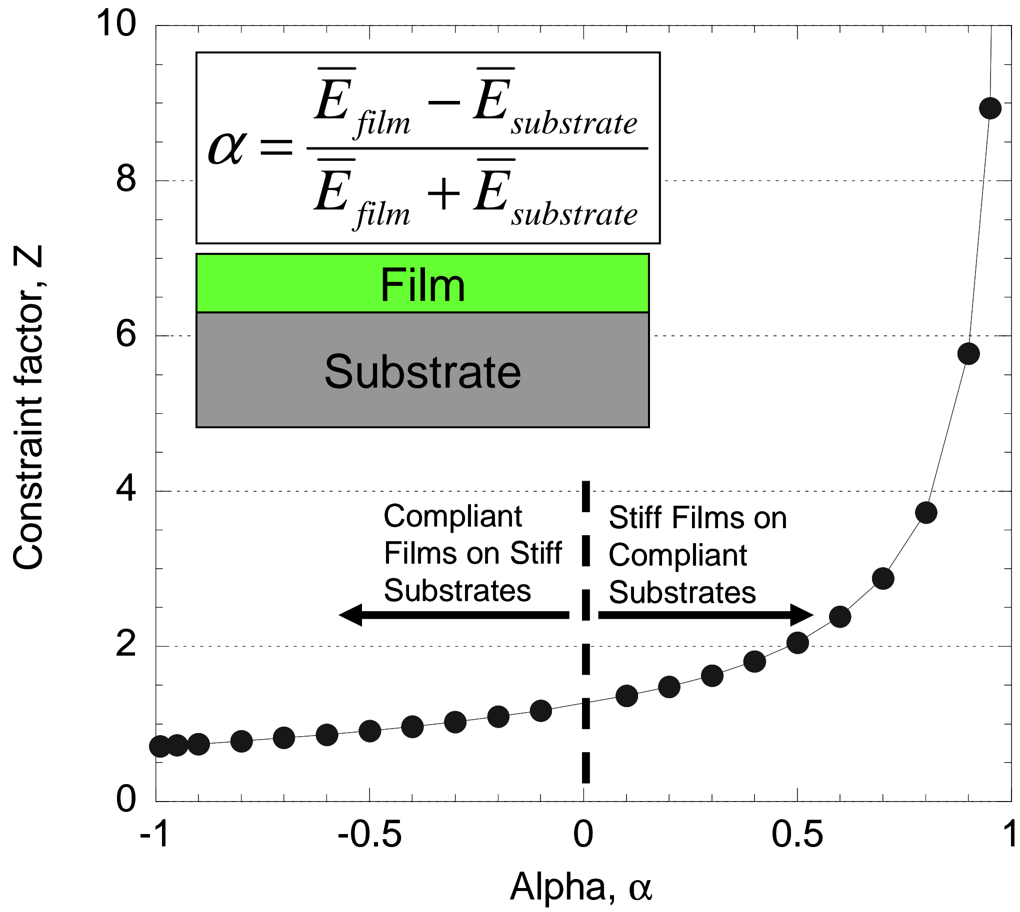

FIG. 1. Plot of the constraint factor (Z) as a function of Dundurs parameters, α and $\beta = \alpha/4$ [7].

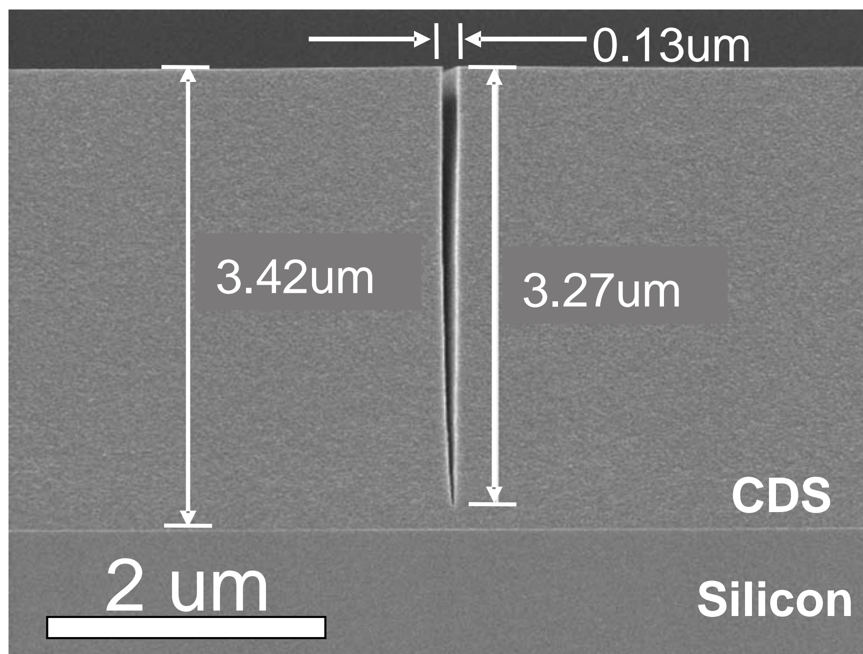

FIG. 2. A typical cross-section scanning electron micrograph of a CDS channel crack.

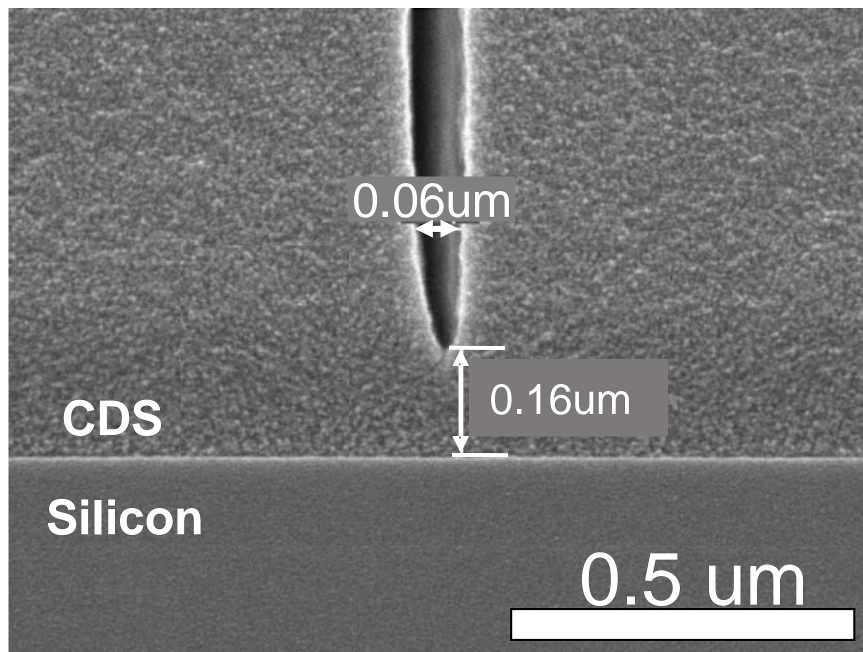

FIG. 3. A high magnification cross-section scanning electron micrograph of a CDS channel crack showing crack termination within the CDS film.

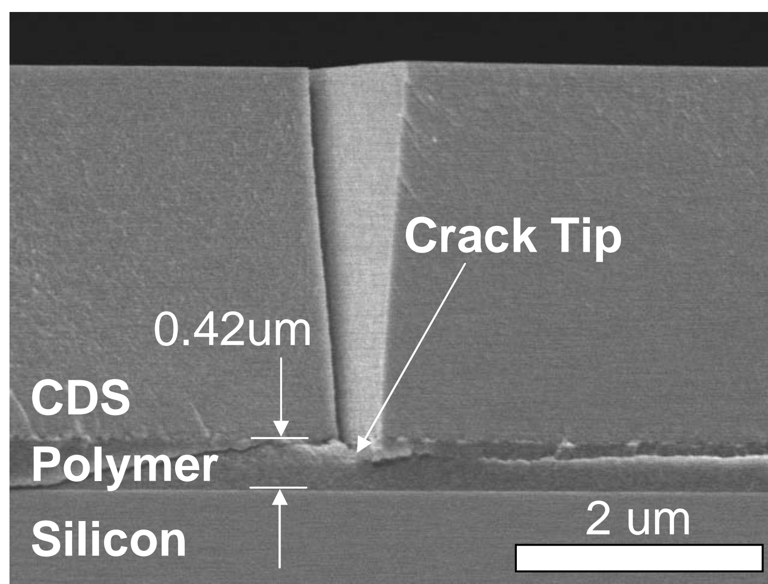

FIG. 4. Cross-section scanning electron micrograph of a channel crack in a CDS film on a silicon substrate with a compliant polymer buffer layer.

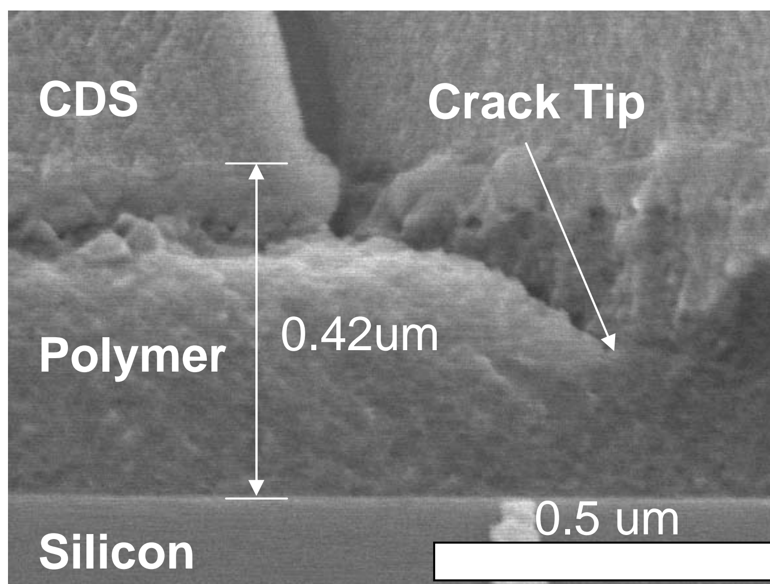

FIG. 5. High magnification cross-section scanning electron micrograph of a CDS channel crack showing its tip terminated in the compliant polymer buffer layer.

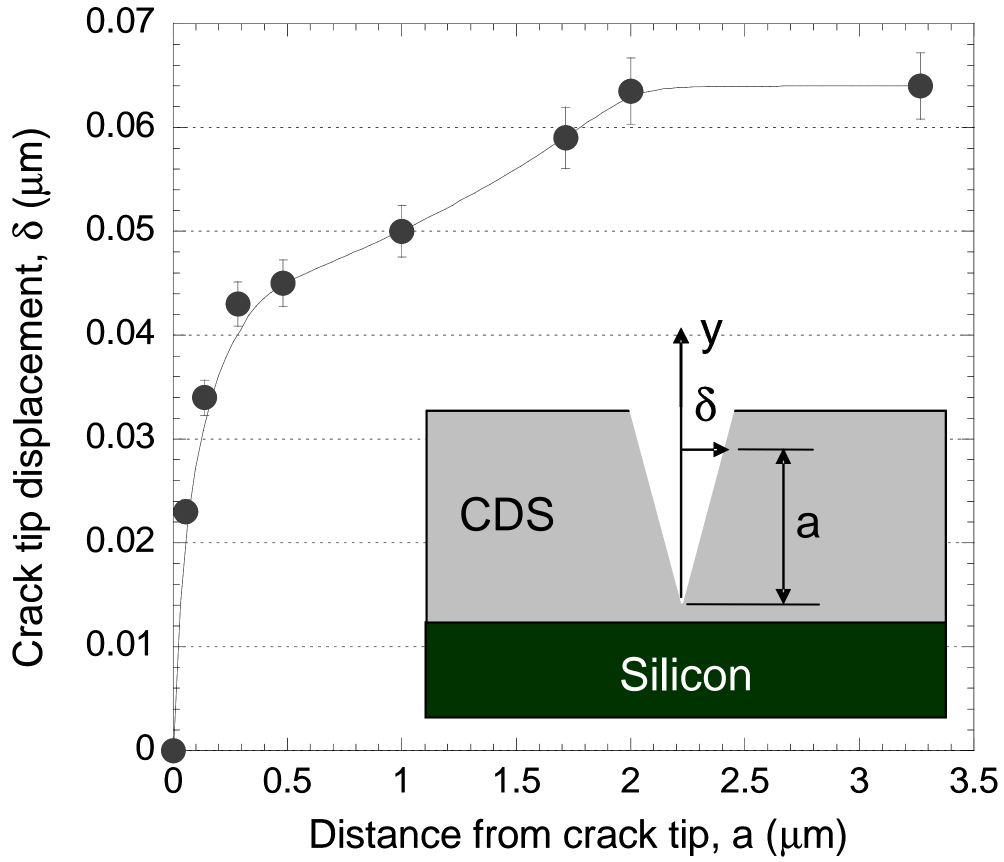

FIG. 6. Plot of crack opening displacement as a function of distance from the crack tip. The scatter bars corresponds to the $\pm$ 5% uncertainty in the SEM magnification.

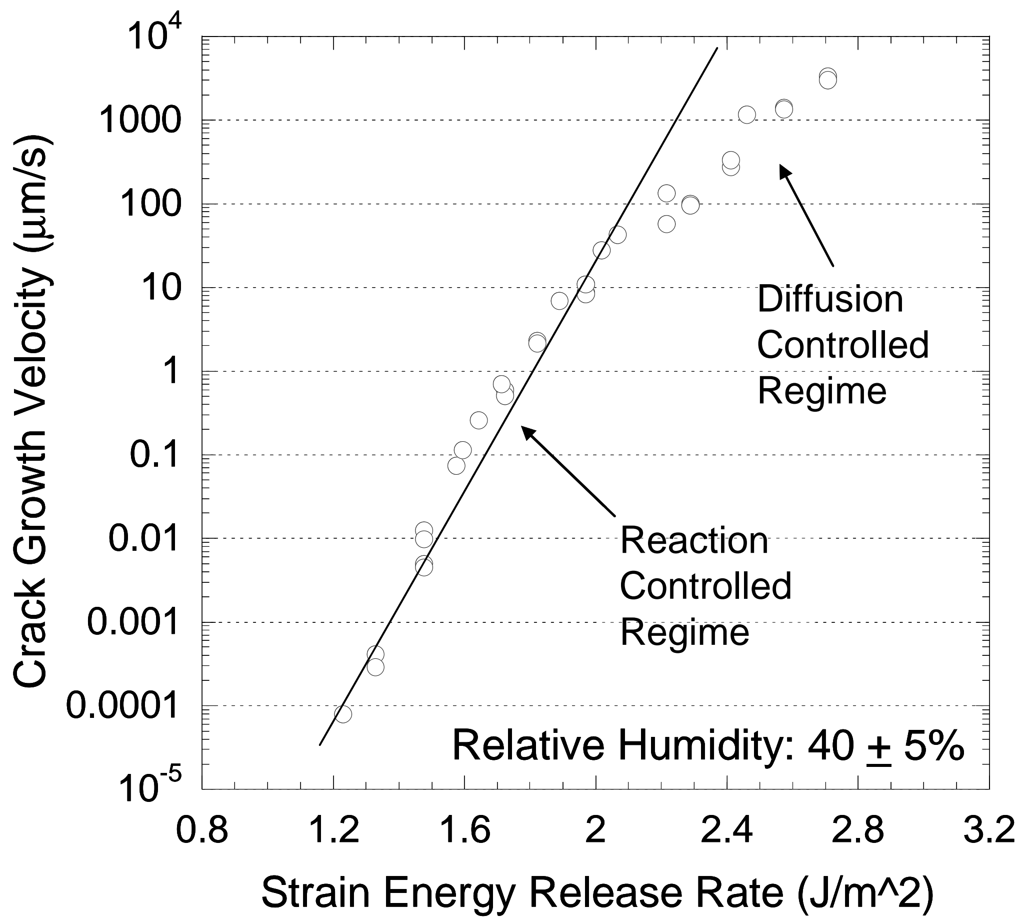

FIG. 7. Plot of CDS crack growth rate as a function of film strain energy release rate calculated using Eq 1.

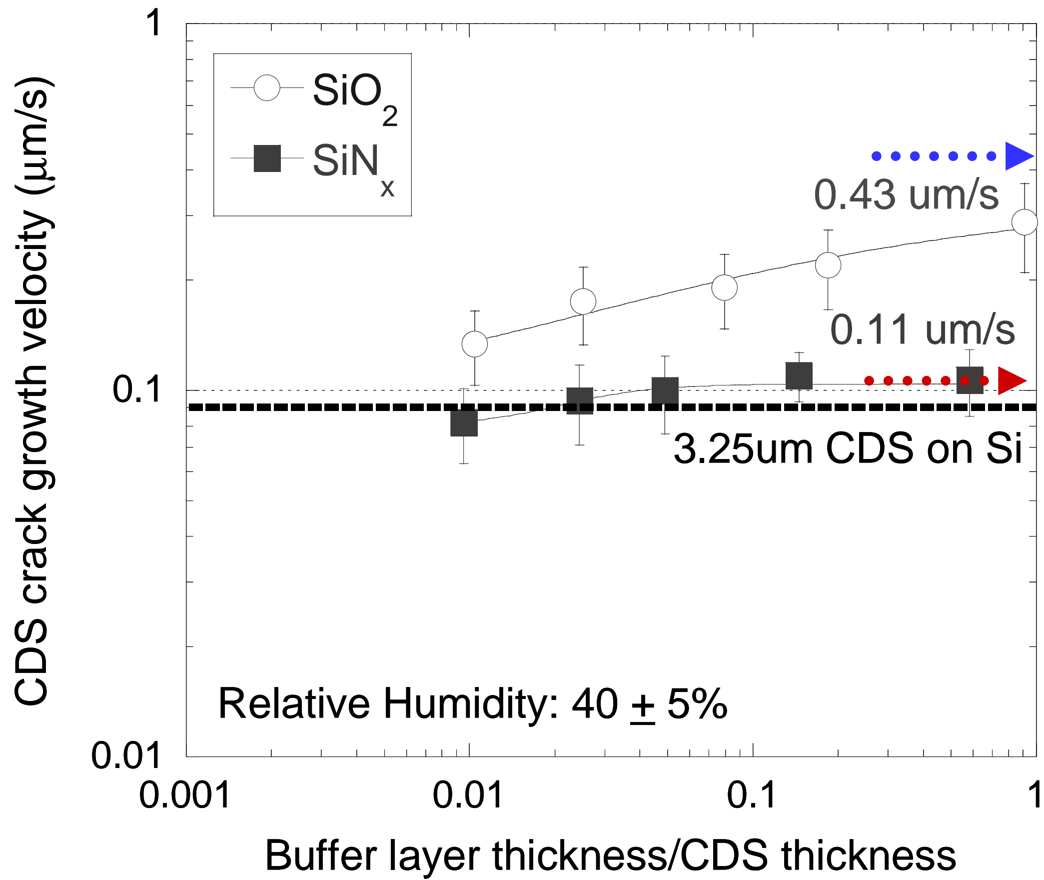

FIG. 8. Plot of CDS crack growth rate as a function of normalized buffer layer thickness.

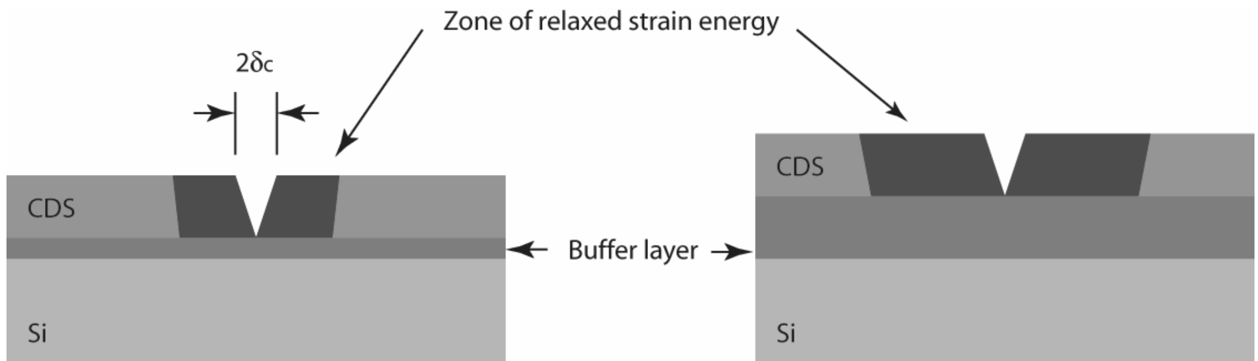

FIG. 9. Schematic drawings of the channel crack elastic zone geometry for samples with thin and thick buffer layer.

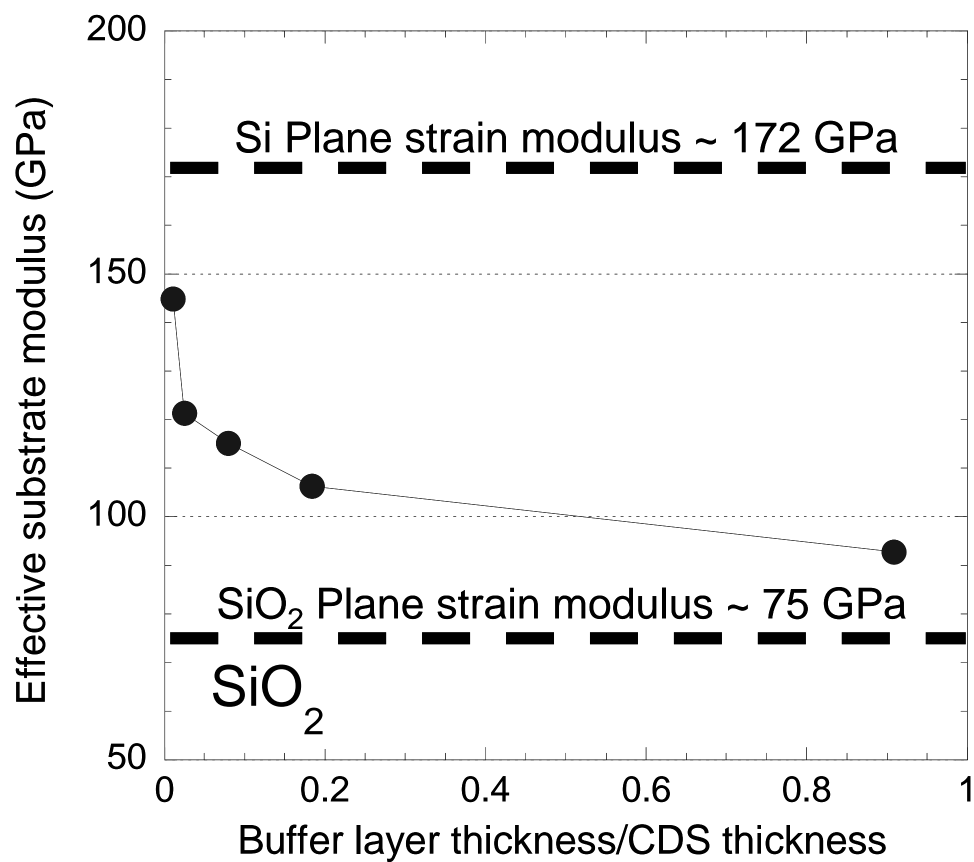

FIG. 10a. Effective substrate modulus of SiO_2 buffer layer sample calculated from the crack growth rate results plotted in Fig. 8.

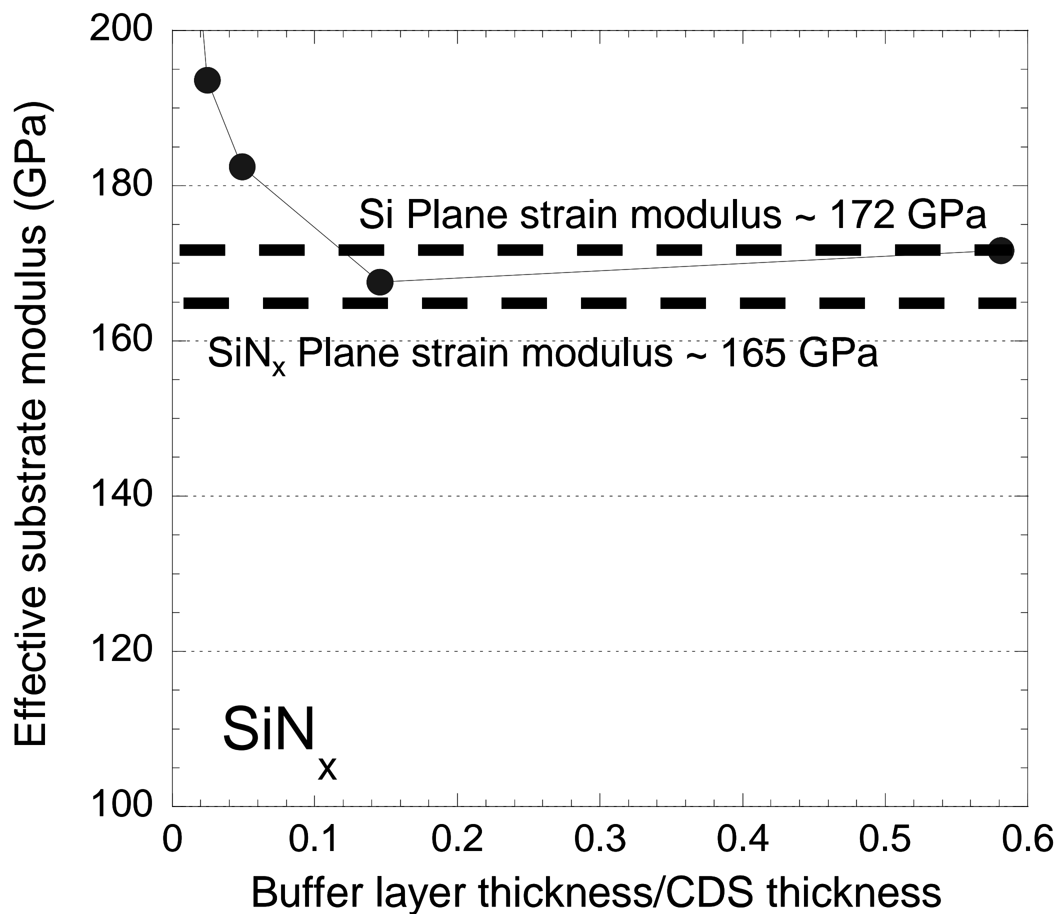

FIG. 10b. Effective substrate modulus of SiN_x buffer layer sample calculated from the crack growth rate results plotted in Fig. 8.

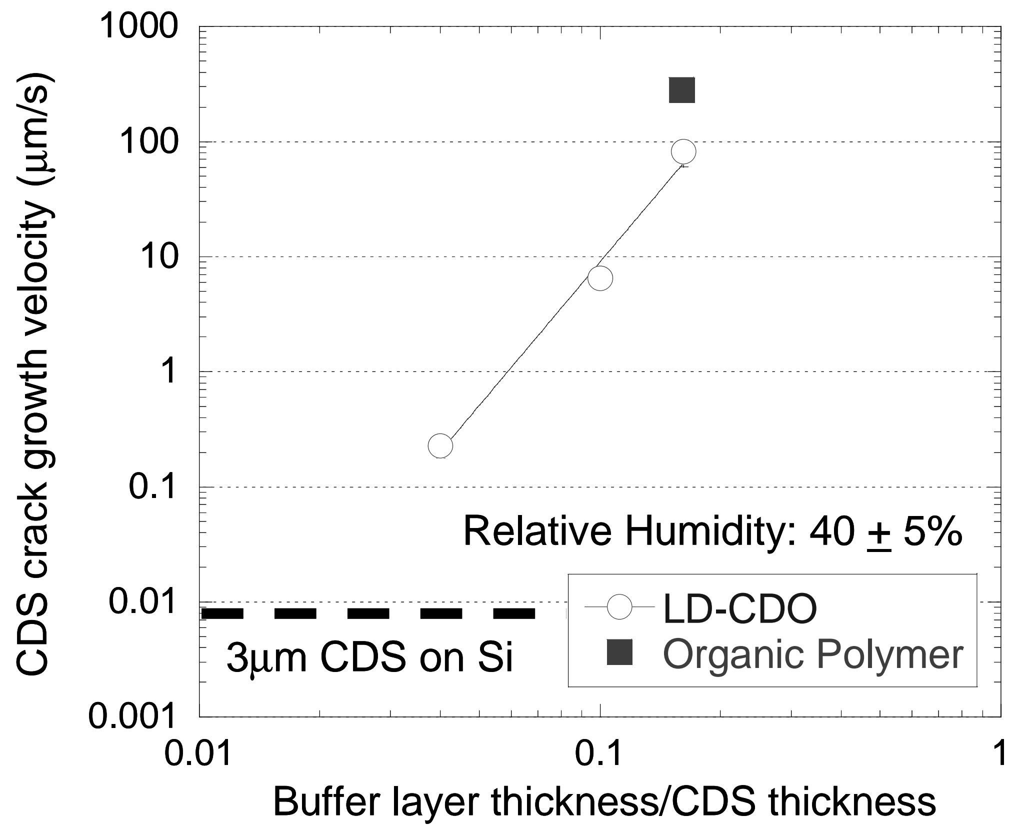

FIG. 11. Plot of CDS crack growth rate as a function of LD-CDO buffer layer thickness.

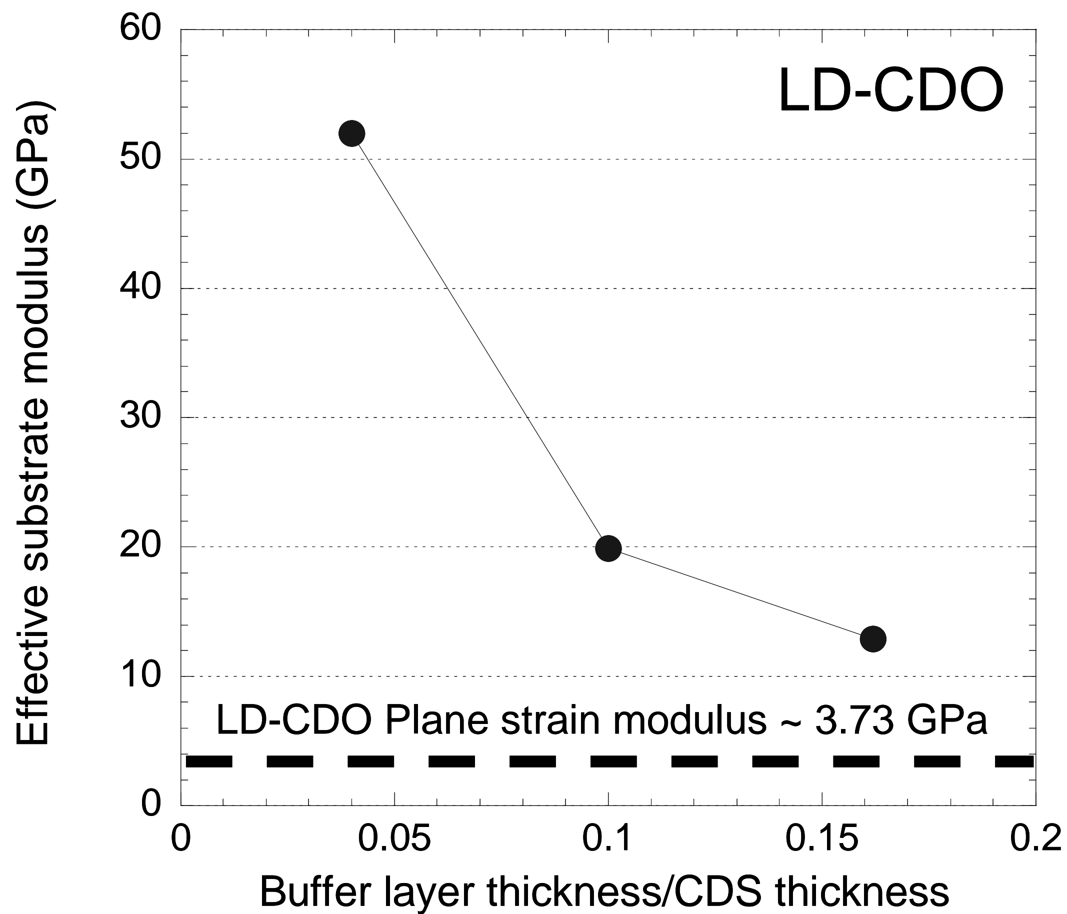

FIG. 12. Effective substrate modulus of LD-CDO buffer layer sample calculated from the crack growth rates plotted in Fig. 11.

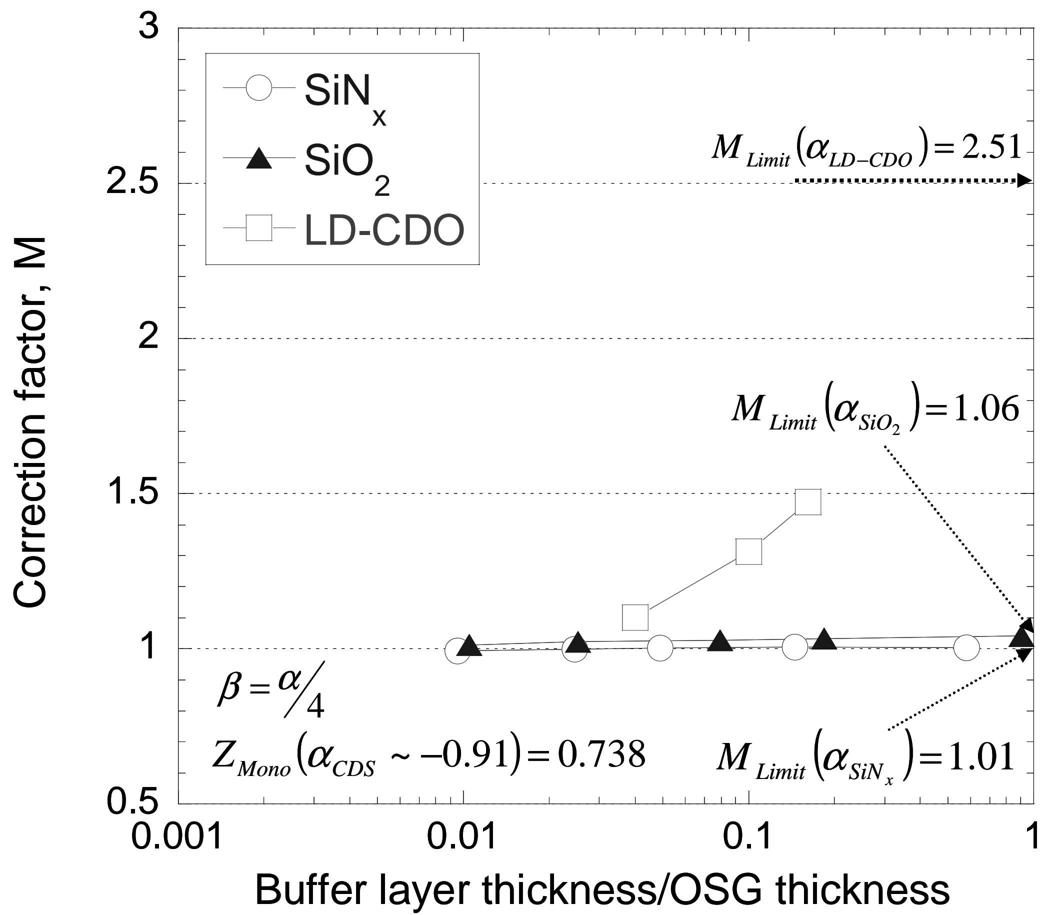

FIG. 13. Plot of correction factor (M) for as a function of buffer layer thickness.

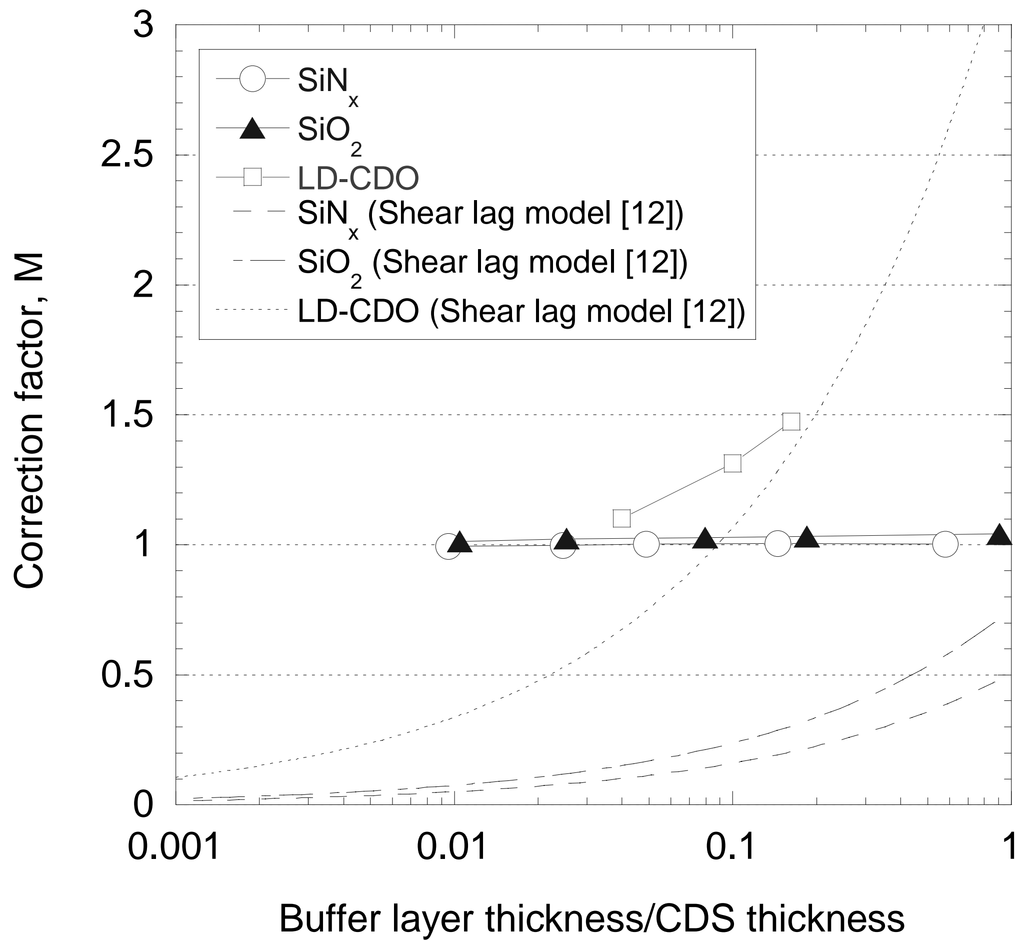

FIG. 14. Comparison between experimental multiplication factors and those calculated from a shear lag model. Symbols represent experimental values; dashed lines are model calculations.